

Isolation and Selection of Radiation Resistant Fungi from Mamuju High Natural Radiation Soil for Uranium and Thorium Bioremediation

N. Robifahmi^{1*}, R. I. Laksana¹, A. A. Pratama¹, A. T. Kusuma¹, T. Tjiptosumirat¹, B. J. Tuasikal¹, E. D. Nugraha¹, M. S. Rijal¹, V. A. Febrian², M. Yusup², W. Futy², A. Mujiyanto², I. Sugoro¹

¹Research Center for Radiation Process Technology, Research Organization for Nuclear Energy (ORTN), National Research and Innovation Agency (BRIN), KST B.J. Habibie Serpong, South Tangerang 15314, Indonesia

²Department of Biology, Science and Technology, UIN Syarif Hidayatullah Jakarta, Jl. Ir H. Juanda No.95, South Tangerang 15412, Indonesia

ARTICLE INFO

Article history:

Received 20 December 2024

Received in revised form 14 March 2025

Accepted 2 March 2025

Keywords:

Radiated soil fungi
Bioremediation
High nature radiation
Mamuju

ABSTRACT

Microorganisms from high natural radiation environments hold potential as bioremediation agents for radioactive waste. In this study, isolation and selection of fungi from Mamuju high natural radiation soil was done for radioactive bioremediation. The methods included fungal isolation from soil samples, radiosensitivity tests, sensitivity tests to uranium and thorium, and absorption tests under gamma radiation (100 Gy hour⁻¹). Results revealed three fungal isolates with high growth ratios and resistance to gamma radiation: *Talaromyces flavus* (A3), *Gongronella butleri* (A4), and *Aspergillus sp.* (F1). Isolates A3 and A4 survived up to 2 kGy, while F1 endured up to 8 kGy. At 24 hours, A3 absorbed uranium at 96% with a biomass of 0.73 g and thorium at 84% with 0.98 g biomass. A4 achieved the highest uranium absorption of 97% (biomass 4.11 g) and thorium absorption of 100% (biomass 0.74 g). F1 demonstrated 96% uranium absorption (biomass 1.29 g) and 87% thorium absorption (biomass 2.17 g). These isolates exhibited significant potential for bioremediation of uranium and thorium-contaminated environments, showing unique adaptations to high radiation conditions and effective radioactive metal uptake.

© 2026 Atom Indonesia. All rights reserved

INTRODUCTION

High natural background radiation is present in our environment and comes from both cosmic and terrestrial sources, such as cosmic rays from outer space and naturally occurring radioactive elements in soil and rocks. Cosmic radiation consists of high-energy particles from outer space, which can penetrate the Earth's atmosphere and contribute to background radiation levels [1]. Terrestrial radiation, on the other hand, arises from naturally occurring radioactive elements such as uranium, thorium, and potassium present in the Earth's crust, which are common in soil, rocks, and air [2]. This natural radiation creates an omnipresent exposure risk,

particularly in areas with high concentrations of these radioactive elements.

Certain areas, such as Ramsar in Iran and Mamuju in Indonesia, exhibit significantly higher levels of terrestrial radiation compared to global averages due to the high concentrations of uranium and thorium in the environment [3,4]. In Mamuju, for instance, annual effective doses can reach up to 32 mSv, making it one of the high natural background radiation (HNBR) areas of global significance [5,6]. These high radiation levels pose both health and ecological risks, necessitating innovative mitigation strategies.

As highlighted by previous studies, microorganisms, including fungi, show promise in managing environments contaminated with radioactive substances. For instance, fungi like *Cryptococcus neoformans* and *Aspergillus niger*

*Corresponding author.

E-mail address: nurr004@brin.go.id

DOI: <https://doi.org/10.55981/aij.2026.1590>

have demonstrated the ability to adapt to high-radiation environments and absorb heavy metals [7,8]. Research on Mamuju residents also revealed alterations in immune biomarkers, such as elevated IgE levels, as an adaptive response to prolonged exposure to natural radiation [9]. These findings emphasize the adaptability of organisms in extreme radiation environments, suggesting potential applications for fungi in remediation efforts.

Exposure to elevated levels of natural radiation poses significant challenges for both human health and environmental sustainability. Studies have linked prolonged exposure to high radiation levels with increased risks of cancer, genetic mutations, and other health disorders, particularly in HNBR areas such as Ramsar and Mamuju [10,11]. At the same time, ecosystems in these areas often experience habitat disruption and potential biodiversity loss due to the accumulation of natural radionuclides [12]. These risks necessitate urgent solutions that integrate ecological sustainability and human health considerations.

In this context, microorganisms, particularly fungi, have emerged as promising candidates for addressing environmental challenges posed by radioactive contamination. Fungi possess unique biological mechanisms, such as biosorption, bioaccumulation, and bioleaching, which enable them to interact with heavy metals and radionuclides, including uranium and thorium solutions [7,8]. Their ability to thrive in extreme environments, including high-radiation areas, further supports their suitability for bioremediation. For instance, *Aspergillus versicolor* has demonstrated a high capacity for biosorption of cobalt-EDTA complexes under acidic conditions, showcasing its potential for managing radionuclide contamination [7]. Similarly, studies on fungal endophytes have revealed their ability to enhance plant growth in contaminated soils, indicating the potential for integrated remediation approaches [13].

Despite these promising capabilities, there remains a significant research gap in understanding the potential of fungi from regions with naturally high radiation, such as Mamuju, Indonesia. Previous studies have predominantly focused on fungi from low to moderate radiation environments [8], leaving the unique characteristics and applications of fungi from HNBR areas underexplored. Addressing this gap is crucial, as fungi from these extreme environments may possess adaptive traits that enhance its bioremediation efficiency. For example, in Takandeang Village, Mamuju, genetic adaptations in the local population exposed to high radiation

have been observed, suggesting the possibility of similar adaptive mechanisms in fungi from this region [14].

To address this gap, this study aims to isolate and identify fungal species from Mamuju's high-radiation soil and evaluate their ability to absorb uranium and thorium solutions under gamma radiation exposure. The findings are expected to reveal fungi with exceptional radiation resistance and metal absorption capabilities. This research contributes to advancing bioremediation technologies for radioactive waste management

METHODOLOGY

This research was conducted at the National Research and Innovation Agency (BRIN) laboratory in Lebak Bulus, South Jakarta. Soil samples were collected from six locations in Mamuju, West Sulawesi: Keang (A), Botteng Kurosalembo (B), Tande-Tande (C), Botteng Tebong (D), Palada (E), and Botteng Batuan (F). The methodology consisted of three main stages: fungal isolation, radiosensitivity testing, metal absorption assays, and molecular identification. These locations were selected based on their potential for uranium and thorium presence. The tools used in this study included an APEL PD-3000 UV spectrophotometer, Petri dishes, 100 mL volumetric flasks, spatulas, 200 μ L microtips, tweezers, 15 mL and 50 mL vials, funnels, glass tubes, a hemocytometer, a microscope (with 40 \times and 100 \times magnification), a shaker, a centrifuge, and an oven. The materials used were Potato Dextrose Agar (PDA), Potato Dextrose Broth (PDB), sodium chloride (NaCl), antibiotics, uranyl acetate ($(\text{CH}_3\text{COO})_2\text{UO}_2 \cdot 2\text{H}_2\text{O}$), thorium nitrate ($\text{Th}(\text{NO}_3)_4 \cdot 5\text{H}_2\text{O}$), ascorbic acid ($\text{C}_6\text{H}_8\text{O}_6$), TOPO (Trioctylphosphine oxide), complex II solution, pH 8.35 buffer, Bromo-PADAP, alcohol, Thorin, and hydrochloric acid (HCl).

Soil sample isolation

Soil samples from the six locations were processed by adding antibiotics to sterilized PDA media, providing optimal growth conditions for fungi. Macroscopic observations included color, texture, and growth patterns, while microscopic observations analyzed hyphae structures, spores, and sporangium using a microscope. Molecular identification was carried out using Polymerase Chain Reaction (PCR) and DNA sequencing.

Radiosensitivity test

The fungal isolates were exposed to gamma radiation using a dose rate of 7 kGy per hour, delivered through the BRIN Gamma Chamber Irradiator. To achieve each desired dose (1 kGy, 2 kGy, 4 kGy, 8 kGy, and 12 kGy), the exposure times were calculated as approximately 8 minutes and 34 seconds for 1 kGy, 17 minutes and 8 seconds for 2 kGy, 34 minutes and 17 seconds for 4 kGy, 68 minutes and 34 seconds for 8 kGy, and 102 minutes and 51 seconds for 12 kGy. Radiosensitivity was assessed by growing fungal isolates on PDA media with and without NaCl and subjecting them to the varying radiation doses. Fungal survival and inhibition were then monitored over a 7-day incubation period. This detailed time calculation ensured accurate and consistent delivery of radiation doses across all samples.

Selection for fungal sensitivity to metals

Based on the evaluation of microbial radiosensitivity, three isolates that showed survival at high radiation doses and had low inhibition were selected. The next process involved preparing a solution of uranium, thorium at a concentration of 10000 ppm in a 100 mL volumetric flask. For each treatment, 60 mL of Potato Dextrose Broth (PDB) was prepared containing eight different doses, for the two types of metals, and applied to three different isolates. Uranium used in the form of uranyl acetate ($(\text{CH}_3\text{COO})_2\text{UO}_2 \cdot 2\text{H}_2\text{O}$), thorium nitrate ($\text{Th}(\text{NO}_3)_4 \cdot 5\text{H}_2\text{O}$).

After preparation of 60 mL of PDB, a 1 mL sample of each solution was taken according to the prescribed treatment dose (0, 50, 100, 200, 400, 600, 800, 1000 ppm). All materials were sterilized, and the antibiotics were added to the Post-sterilized PDB. Then, uranium, thorium solutions were added according to the predetermined treatment doses. The solution was then poured into Petri dishes and allowed to solidify for one day. Isolates A3, A4, and F1 were prepared, cut into slices, and planted on PDA media that had been treated with metals. Fungal growth was observed for seven days.

Absorption of metals by selected fungi under gamma irradiated conditions

The fungal isolate was mixed with 10 mL of NaCl solution, then rubbed using a rose and put into a 15 mL vial using a funnel. The number of spores was counted using a hemocytometer under a microscope. A total of 1 mL of spore suspension

was put into a 50 mL vial containing 20 mL of Potato Dextrose Broth (PDB) medium and shaken at 100 rpm for 3 days. After incubation, 2.40 mL of culture was taken from a total of 20 mL of PDB and added to uranium and thorium solutions at a concentration of 400 ppm according to the treatment exposure times of 0, 4 hours, and 24 hours.

The culture was then irradiated at IRPASENA (Irradiator Panorama Serbaguna) with a dose rate of 100 Gy for 4 and 24 hours. Empty bottles were prepared to hold the pellets and supernatants. The supernatant was separated and put into a glass vial, while the pellet was transferred into a 15 mL vial according to the exposure time treatment. The samples were centrifuged for 10 minutes at 5000 rpm, then the supernatant was transferred to a glass vial and the pellet to a 15 mL plastic vial. The pellets were oven-dried for 1 day, then weighed to calculate the biomass. The pellet condition was left open, while the pH of the supernatant was measured and then stored in the freezer. The absorption data were analyzed statistically using Microsoft Excel, where descriptive statistics were used to summarize the data, and graphs were generated to visualize trends in fungal absorption efficiency under different irradiation and metal concentrations.

Uranium metal sorption test

A total of 1 mL of sample solution was pipetted into a shake flask, then 2 mL of 5% ascorbic acid and 5 mL of 0.05 N TOPO solution were added. The solution was shaken for 2 minutes and left until the organic phase separated well from the aqueous phase. After separation, 2 mL of the organic phase was pipetted and put into a 25 mL volumetric flask. Next, 1 mL of complex II solution, 1 mL of pH 8.35 buffer solution, and 2 mL of 0.05% Bromo-PADAP solution were added. After 10 minutes, alcohol was added until the volume of the solution was exactly 25 mL. For the preparation of the blank, 2 mL of TOPO was pipetted into a 25 mL volumetric flask, and the same reagents as numbers 2 to 3 were added. Uranium complex solution with Bromo-PADAP was allowed to stand for at least 30 minutes, after which the absorbance was measured with a spectrophotometer at a wavelength of 574 nm.

Thorium metal sorption test

First, tools and chemicals were prepared. A 0.1% Thorin solution was made by dissolving 1 gram of Thorin in 1 L of HCl, pH 0.8. A 5% ascorbic acid solution was made by dissolving 5 g of

ascorbic acid in 100 mL of distilled water. HCl pH 0.8 solution is made by adding HCl little by little into distilled water until it reaches pH 0.8. To make the thorium standard calibration curve, thorium standard solutions with concentrations of 5, 10, 25, 50, 100, 150, and 200 ppm were pipetted into a 50 mL volumetric flask. Then, 5 mL of 5% ascorbic acid and 5 mL of 0.1% Thorin solution were added to each flask. The solution volume was adjusted with HCl to pH 0.8.

After 30 minutes, the absorbance of the thorium complex solution with Thorin was measured using a spectrophotometer at a wavelength of 545 nm to obtain thorium standard calibration curve data. For sample testing, 1 mL of sample solution containing thorium was pipetted into a 50 mL volumetric flask. 5 mL of 5% ascorbic acid and 5 mL of 0.1% Thorin solution were added. The solution volume was adjusted with HCl to pH 0.8. After 30 minutes, the absorbance of the thorium complex solution with Thorin was measured using a spectrophotometer at a wavelength of 545 nm.

Molecular identification

Molecular identification is carried out by the Sanger DNA Sequencing method using Capillary Electrophoresis to read the isolated DNA sequence. This method provides accurate results by separating DNA fragments based on size. This approach helps ensure precise species identity in the identification process of microorganisms. The sequence data were analyzed using MEGA (Molecular Evolutionary Genetics Analysis) software to perform sequence alignment and phylogenetic analysis, ensuring accurate identification and classification of fungal isolates.

RESULTS AND DISCUSSION

Physico-chemical characteristics of soils from sites with high natural radiation in Mamuju

Based on data from Table 1, Mamuju soils were selected for their potential uranium and

thorium presence. Radiation dose rates at sampling sites ranged from 100 $\mu\text{Sv hour}^{-1}$ in Keang to 8000 $\mu\text{Sv hour}^{-1}$ in Botteng Batuan, with Botteng Kurosalembo, Tande-Tande, Botteng Tebong, and Palada showing intermediate levels. Prior studies confirmed high uranium (^{238}U) and thorium (^{232}Th) concentrations, with Rosianna et al. (2023) reporting averages of 22.88 Bq kg^{-1} for uranium and 33.54 Bq kg^{-1} for thorium, particularly in laterite and rocks [6].

These soil physico-chemical conditions are key factors that influence the diversity and survival of microorganisms in extreme environments. Various studies have shown the importance of soil physico-chemical characteristics in supporting the growth of microorganisms in extreme environments. Sites such as Tande-Tande, Botteng Kurosalembo, and Botteng Tebong have neutral soil pH and sufficient organic matter content, which allows the growth of microorganisms such as *Aspergillus niger* [15], *Deinococcus radiodurans*, [16], and *Rubrobacter* [17] emphasized that microorganisms that survive in highly irradiated soils have special adaptation mechanisms, while Neina (2019) added that soil pH plays an important role in determining the distribution of microorganisms [18].

These adaptations not only allow microorganisms to survive in extreme conditions but also provide great opportunities for their utilization. Microorganisms that are able to adapt to soils with high radiation have great potential in bioremediation technology [19]. Billi et al. (2019) [20] also reported that extremophilic microorganisms play an important role in cleaning up heavy metal contamination and radiation. Recent research supports that the adaptation of microorganisms to extreme conditions makes them ideal candidates for bioremediation technology. With these adaptations, microorganisms in Mamuju have significant potential to serve as an effective solution for addressing radioactive contamination in the environment [21].

Table 1. Physico-chemical characteristics of soils from Mamuju high-radiation sites, including radiation dose ($\mu\text{Sv/h}$), pH, organic matter content (%), and soil moisture (%), which influence fungal survival and bioremediation potential.

Parameters	Unit	Keang	Kurosalembo Botteng	Tande-Tande	Botteng Tebong	Palada	Rock Botteng
Radiation dose	$\mu\text{Sv/hour}$	100	600	1500	2500	2500	8000
Water content	%	25.76	46.28	39.56	43.49	40.10	4.10
Dry material	%	74.23	53.71	60.43	56.60	59.89	95.80
Ash material	%	94.53	84.28	81.13	86.32	86.46	91.40
Organic matter	%	5.46	15.71	18.86	13.67	13.53	8.50
pH		7.03	5.65	7.35	7.21	7.21	8.01
C-organic	%	0.69	1.63	1.55	1.78	0.14	0.25
N-total	%	0.14	0.19	0.16	0.17	0.06	0.06
C/N Ratio	%	4.87	8.40	9.71	10.32	2.32	4.18

Macroscopic and microscopic morphological characteristics of fungal isolates from high natural radiation soil in Mamuju

Based on Table 2, 17 fungal isolates were obtained from various locations in Mamuju, exposed to high natural radiation. These fungal isolates were taken from several locations such as Keang, Botteng Kurosalembo, Tande-Tande, Botteng Tebong, Palada, and Botteng Batuan. Observations were made of macroscopic morphology, which included color, texture, and colony growth patterns. In addition, microscopic morphology, such as spore size, hyphal structure, and the presence of sporangium, which is the bag or place of spore formation, was also observed. The results of these observations show that the physico-chemical conditions of the soil at each location are different, which affects the growth of fungal isolates in that environment.

Externally visible differences, such as the size and shape of fungal colonies, indicate the possibility of changes inside the fungi, such as in the spores and hyphae. These changes help the fungi adapt to challenging environments, such as soil exposed to high radiation. Some isolates grow faster, while others have

irregular colony edges, as a form of adaptation to extreme conditions. Morphological diversity in *Flavi's Aspergillus* section indicates an adaptive response to unusual environmental conditions [22].

This adaptation is further supported by microscopic observations of isolates from high-radiation soil in Mamuju, as shown in Figs. 1(a,b). These observations reveal spores, strongly branched hyphae, and sporangium structures that protect the spores. Such structures enhance the fungi's ability to survive under high radiation conditions. Isolates such as *Aspergillus sp.* and *Penicillium sp.* have well-developed hyphae, allowing them to grow in soils exposed to radiation [15,24].

Overall, this study shows that fungal isolates from highly irradiated soil in Mamuju have unique morphological characteristics, both macroscopically and microscopically. The adaptations seen in colonies, spores, hyphae, and sporangium suggest that these fungi have developed specialized mechanisms to survive in extreme conditions. These findings open up great opportunities for bioremediation applications, particularly in the treatment of radiation-contaminated environments.

Table 2. Morphological characteristics of fungal isolates from Mamuju high natural radiation soil.

Code	Location	Surface color	Colony back color	Margin	Texture	Elevation	Mycelium	Exudates	Diameter (7 HI)	Growth
A1R	Keang	White, grayish, yellow	Yellow brown	Filamentous	Velvet	Raised	Aerial	+	5.5 cm	Quick
A1S		White	Light yellow	Filamentous	Velvet	Raised	Aerial	+	6 cm	Quick
A2		Intense white	Yellowish white	Filamentous	Velvet	Umbonate	Aerial	-	2.5 cm	Quick
A3		Yellowish white	Yellow white	Filamentous	Velvet	Raised	Aerial	-	6 cm	Quick
A4		Greenish white	Yellowish brown	Filamentous	Velvet	Raised	Aerial	+	6 cm	Quick
A5		Yellow	Yellow	Filamentous	Velvet	Raised	Aerial	+	6.5 cm	Quick
B1Y	Kurosalembo Botteng	Yellow, black	Yellow, black	Undulate	Rough	Raised	Aerial	+	1 cm	Quick
B2		White	Yellow	Filamentous	Velvet	Raised	Aerial	-	4 cm; 6 cm	Quick
B3		Ash white	Yellow	Filamentous	Velvet	Raised	Aerial	-	3.5 cm	Quick
C3	Tande-Tande	White, purple	Yellow	Filamentous	Velvet	Raised	Aerial	-	2.5; 3.5 cm	Quick
C1D		White, green	Yellow	Filamentous	Velvet	Raised	Aerial	+	10 cm	Quick
C2Y		Yellow	Yellow	Filamentous	Velvet	Raised	Aerial	+	2.6 cm	Quick
E2		White, ash	Yellow	Filamentous	Velvet	Raised	Aerial	-	3.5 cm	Quick
E3		White, ash	Yellow	Filamentous	Velvet	Raised	Aerial	-	4.5 cm	Quick
E1Y	Palada	White, yellow	White, Yellow	Undulate	Rough	Umbonate	Aerial	-	1 cm	Quick
E1R2Y		White, yellow	White, Yellow	Undulate	Rough	Umbonate	-	-	1 cm	Quick
F1	Rock Botteng	Ash, blackish	Ash, Yellowish	Filamentous	Velvet	Raised	Aerial	-	7.5 cm	Quick



Fig. 1. Microscopic observations of fungal isolates from Mamuju high natural radiation soil. (a) Spores and hyphae of isolates A3 and A4; (b) Sporangium structure of isolate F1, which plays a role in spore protection under radiation exposure.

Fungal radiosensitivity test

The fungal radiosensitivity test revealed notable differences in the ability of isolates to withstand gamma radiation, as shown in Table 3. Isolates A3 and A4 demonstrated strong growth at doses up to 2 kGy, while isolate F1 exhibited exceptional resistance, continuing to grow even at doses as high as 8 kGy with the addition of NaCl. In contrast, isolate E1Y showed limited growth at 2 kGy and a significant decline at 4 kGy, indicating weaker adaptability to radiation-induced stress.

This resilience in A3 and A4 is attributed to their enhanced DNA repair mechanisms and metabolic adaptations, which mitigate the harmful effects of gamma radiation [25]. Additionally, growing media with or without NaCl affects the resistance of fungi to radiation. Fungi without NaCl generally grow better after radiation exposure, especially at low doses, because they are not burdened by salt stress and can focus more on overcoming the effects of radiation. High concentrations of NaCl impose significant osmotic and oxidative stress on fungi, inhibiting growth and reducing their ability to respond effectively to additional stressors like radiation [26]. Moreover, the higher water content in cells in fungi without NaCl helps to protect cells from radiation damage [25,26]

These findings highlight the superior adaptability of isolates A3, A4, and F1 and their potential applications in the bioremediation of radiation-contaminated environments. Their ability to survive under extreme radiation conditions, especially in optimized environments, makes them promising candidates for future research and practical implementation in bioremediation, particularly for managing and restoring ecosystems affected by radioactive pollution.

Sensitivity evaluation of selected fungi to uranium and thorium metals

Based on the data in Table 4, the sensitivity evaluation of three fungal isolates (A3, A4, and F1) to various concentrations of uranium and thorium metals is shown. In general, the growth of the three isolates decreased as uranium and thorium concentrations increased, but with different levels of tolerance. These differences in tolerance between the three isolates indicate variations in the fungi's adaptation mechanisms to heavy metal stress. Fungal growth is marked with "+" to "++++", describing growth rates from severely inhibited to excellent, while "-" signifies no growth or very high sensitivity to uranium.

Table 3. Growth ratio of fungal isolates exposed to gamma radiation at different doses (1-12 kGy) under NaCl and non-NaCl conditions. Growth levels are categorized as: +++++ (very good), ++++ (good), +++ (moderate), ++ (low), + (very low), - (no growth).

Isolate Code	1 kGy		2 kGy		4 kGy		8 kGy		12 kGy	
	NaCl	Non NaCl	NaCl	Non NaCl	NaCl	Non NaCl	NaCl	Non NaCl	NaCl	Non NaCl
AIR	+++	++++	+++	+++	-	-	-	-	-	-
AIS	+++	+++	++++	+++	-	-	-	-	-	-
A2	+++	+++	+	+	-	-	-	-	-	-
A3	++++	++++	++++	++++	-	-	-	-	-	-
A4	++++	++++	+++	++++	-	-	-	-	-	-
A5	+++	++	+++	++	-	-	-	-	-	-
B1Y	-	-	-	-	-	-	-	-	-	-
B2	+++	++++	++	+++	-	-	-	-	-	-
B3	++++	+++	-	+	-	-	-	-	-	-
C3	++++	++++	-	-	-	-	-	-	-	-
CID	-	-	-	-	-	-	-	-	-	-
C2Y	++++	++++	+++	++++	-	++	-	-	-	-
E2	+	++	-	-	-	-	-	-	-	-
E3	++	+++	-	-	-	-	-	-	-	-
E1Y	+++	++++	+++	++++	+++	++++	-	-	-	-
E1R2Y	+++	+++	-	-	++	-	-	-	-	-
F1	+++	+++	++++	+	+	-	+	+	-	-

Table 4. Sensitivity evaluation of fungal isolates (A3, A4, and F1) to uranium and thorium metals at different concentrations (0-1000 ppm). Growth is classified as +++++ (excellent), ++++ (good), +++ (moderate), ++ (low), + (very low), and - (no growth).

Isolate	Uranium dose (ppm)							
	0	50	100	200	400	600	800	1000
A3	++++	++++	+++	+++	++	+	+	+
A4	++++	+++	+++	++	++	+	+	+
F1	++++	++++	++++	++++	++++	++++	++++	++
Isolate	Thorium dose (ppm)							
	0	50	100	200	400	600	800	1000
A3	++++	++++	++++	++++	++	+	-	-
A4	++++	++++	++++	++++	+++	+++	++	-
F1	++++	++++	++++	++++	++++	++++	+++	+

Isolates A3 and A4 exhibited strong biosorption capacities for uranium, supported by antioxidant activity and chitin-rich cell walls, although their growth declined notably at 400 ppm. Defense mechanisms such as antioxidant production enabled A3 to mitigate oxidative stress caused by uranium exposure, as also observed in studies on *Candida utilis*, which increased antioxidant activity to minimize oxidative damage [27]. Similarly, A4 demonstrated slightly better resistance to uranium and thorium due to enhanced biosorption mechanisms and enzymatic activity, consistent with findings on *Penicillium janthinellum*, which uses antioxidant enzymes and transporters to tolerate heavy metals [28].

Meanwhile, isolate F1 exhibited the highest tolerance, maintaining stable growth up to 1000 ppm for both uranium and thorium. This superior tolerance is attributed to effective defense mechanisms, including biosorption, bioreduction of uranium into less harmful forms, and the production of protective compounds like melanin. Melanin in fungal cell walls not only binds heavy metals such as uranium and thorium but also protects cells from their toxic effects. Studies on fungi like *Talaromyces*, *Penicillium*, and black fungi such as *Exophiala mesophila* highlight the role of melanin in mitigating heavy metal toxicity while enhancing fungal survival in extreme environments [29-32]. These findings underscore the potential of these isolates for bioremediation in environments contaminated with uranium and thorium.

Absorption of uranium and thorium metals and biomass changes of selected fungi under gamma-irradiated conditions

The data in Fig. 2 showed that fungal isolates A3, A4, and F1 from soil exposed to high radiation in Mamuju exhibit different abilities to absorb uranium and thorium under gamma radiation exposure. These fungi tend to absorb uranium more effectively because uranium dissolves more easily in water as UO_2^{2+} ions, while thorium tends to form insoluble compounds like ThO_2 [33]. Gamma radiation exposure can also trigger changes in the fungal cell wall, such as an increase in active functional groups (carboxyl, hydroxyl, amino) and polysaccharide composition (chitin, glucan), enhancing the fungi's ability to bind uranium [34].

Comparison of fungal absorption rates and biomass changes under uranium and thorium exposure is illustrated in Fig. 2(a) shows uranium absorption percentage over 24 hours, while Fig. 2(b) depicts thorium absorption percentage over 24

hours. Changes in biomass for uranium-exposed fungi are presented in Fig. 2(c), and Fig. 2(d) illustrates biomass changes in fungi exposed to thorium. Absorption efficiency and biomass were measured in % and g, respectively.

In addition, isolate A3 showed a high uranium uptake capacity, reaching 95-96% in 24 hours, although the biomass decreased from 0.73 g to 0.26 g. This decrease in biomass is caused by the toxicity of uranium, which inhibits growth and damages fungal cells, disrupting metabolic processes. This result is in line with the research of Ahmed (2021), which states that high uranium concentrations can inhibit fungal growth [33]. In thorium absorption, isolate A3 experienced an increase in biomass from 0.19 g at hour 0 to 0.98 g at hour 24, with thorium absorption reaching 84.24%. This increase may be due to the ability of isolate A3 to adapt to thorium exposure through the production of protective and metal-binding compounds, which help neutralize its toxic effects and utilize nutrients more efficiently.

Then, isolate A4 showed differences in uranium and thorium uptake. When absorbing uranium, isolate A4 increased from 94.60% to 97.40% in 24 hours, with biomass rising from 0.34 g to 4.10 g. This happened because the fungi used uranium as an energy source, converting it from a toxic to a safer form with the help of enzymes, thus supporting their growth and increasing their biomass. On the contrary, when absorbing thorium, although the absorption reached 100%, the biomass decreased from 0.74 g to 0.19 g. This occurs due to the higher stability of thorium and is difficult to decompose, so the fungi must spend more energy to deal with the damaging effects of thorium exposure, such as cell damage and metabolic disorders. Fungi can produce protective compounds to reduce damage from heavy metals, but this process requires energy, which can inhibit the growth of fungi if the toxicity level of the metal is high.

Furthermore, isolate F1 showed good adaptation to uranium and thorium. Under conditions with uranium, F1 biomass increased from 0.60 g to 1.29 g in 24 hours, presumably due to its ability to utilize other nutrients more efficiently. On exposure to thorium, the F1 isolate achieved 86.52% uptake, with biomass increasing to 2.17 g. This increase may be due to F1's ability to produce protective and metal-binding compounds, helping the fungus deal with the initial damage from heavy metal exposure. Research by Jiménez-Gómez *et al.* (2022) supports these findings, suggesting that fungi can produce heavy metal-binding compounds to protect their cells [26]. With this adaptability, isolates A3, A4, and F1 have strong potential for use in the bioremediation of heavy metal and radiation-contaminated environments.

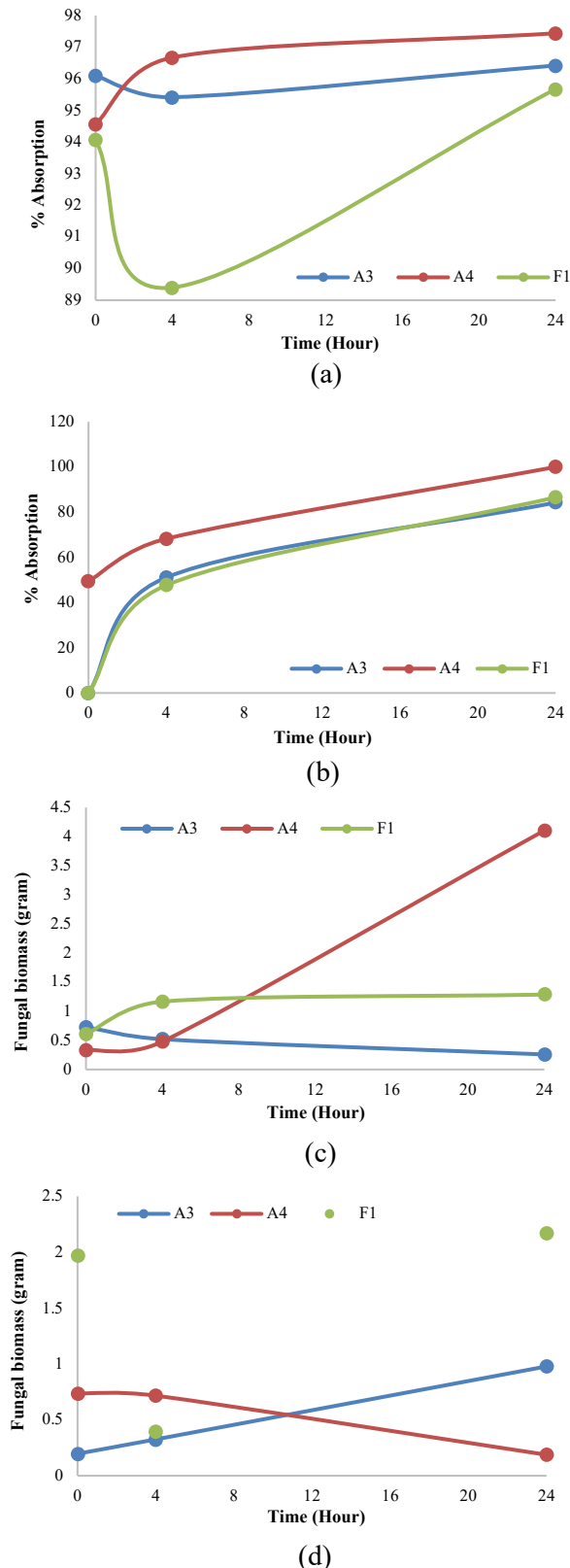


Fig. 2. Comparison of fungal absorption rates and biomass changes under uranium and thorium exposure: (a) Uranium absorption percentage over 24 hours; (b) Thorium absorption percentage over 24 hours; (c) Biomass changes in uranium-exposed fungi; and (d) Biomass changes in thorium-exposed fungi. Absorption efficiency and biomass were measured in % and g, respectively.

Fungi bioremediate heavy metals through biosorption, bioaccumulation, and precipitation, where metals bind to cell walls, are absorbed, or form less toxic complexes. Their resistance mechanisms include detoxifying enzymes (peroxidase, laccase), extracellular polysaccharides, and pH regulation, which help neutralize metal toxicity. These adaptations enable fungi to survive in contaminated environments and play a crucial role in bioremediation efforts [35].

Fungi resist ionizing radiation through oxidative stress defences, melanin absorption, and DNA repair mechanisms like Non-Homologous End Joining (NHEJ) and Homologous Recombination (HR). Antioxidants such as Superoxide Dismutase (SOD) and catalase help neutralize Reactive Oxygen Species (ROS), while melanin reduces radiation-induced damage. Some fungi also delay cell division or slow growth, enhancing survival and demonstrating their resilience in extreme environments [23].

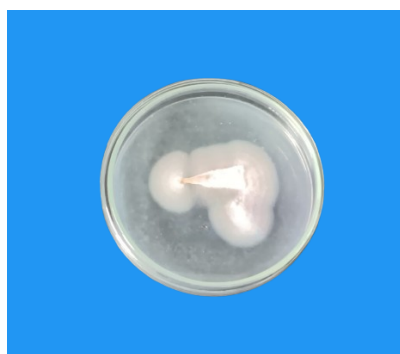
Molecular identification results

The results of molecular identification using the Sanger DNA Sequencing method with Capillary Electrophoresis provide important information about the specific identity of the three fungal isolates studied as summarized in Table 5. Isolate A3 is similar to *Talaromyces flavus* isolate mf-1, isolate A4 is similar to *Gongronella butleri* isolate P1, and isolate F1 is similar to *Aspergillus sp.* isolate MEBP 0049, each with a similarity level of 100%. This perfect degree of similarity demonstrates the accuracy of the identification and provides a strong basis for further understanding of the characteristics and potential of each isolate.

Talaromyces flavus, known to have various biotechnological applications, including potential in bioremediation, represents isolate A3. *Gongronella butleri*, although less common, has been reported to have good adaptability to various environmental conditions, representing isolate A4. Meanwhile, *Aspergillus sp.*, a vast genus of fungi with many species known to have capabilities in bioremediation of heavy metals and other toxic compounds, represents isolate F1. Figure 3 shows the visualization of the three molecularly identified isolates: a) isolate A3 (*Talaromyces flavus* isolate mf-1), b) isolate A4 (*Gongronella butleri* isolate P1), and c) isolate F1 (*Aspergillus sp.* isolate MEBP 0049).

Table 5. Molecular identification results of fungal isolates from Mamuju high-radiation soil. Species names were determined by Sanger sequencing with 100% similarity to reference strains.

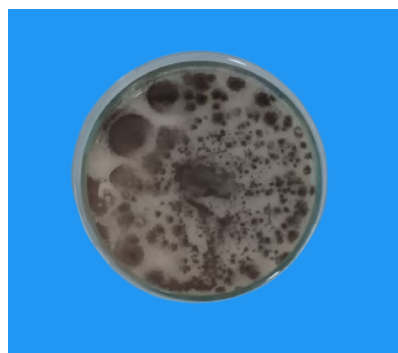
Isolate code	Species Name	Similarities
A3	<i>Talaromyces flavus</i> isolate mf-1	100%
A4	<i>Gongronella butleri</i> isolate P1	100%
F1	<i>Aspergillus</i> sp. isolate MEBP 0049	100%



(a)



(b)



(c)

Fig. 3. Molecular identification of fungal isolates based on Sanger sequencing. (a) *Talaromyces flavus* isolate mf-1 (A3); (b) *Gongronella butleri* isolate P1 (A4); and (c) *Aspergillus* sp. isolate MEBP 0049 (F1). Identification was based on 100% sequence similarity with reference strains.

CONCLUSION

Fungal isolates A3, A4, and F1 showed strong potential for bioremediation in environments contaminated with radiation from uranium and thorium. Isolate A3 and isolate A4 survived up to 2 kGy, while isolate F1 survived up to 8 kGy. Isolate F1

showed the highest tolerance to uranium and thorium solutions at 1000 ppm, with isolate A4 achieving 97.44% uranium uptake and isolate F1 86.52% thorium uptake. Molecular identification revealed 100% genetic similarity among the three isolates, with isolate A3 identified as *Talaromyces flavus*, isolate A4 as *Gongronella butleri*, and isolate F1 as *Aspergillus* sp. These results emphasize the potential of these fungal isolates in radioactive waste bioremediation. To advance toward practical applications, further research is needed, including field trials, genetic studies, and multi-metal contamination assessments under various soil conditions.

ACKNOWLEDGMENT

The authors would like to thank the Budget Implementation (DIPA) of the Research Organization for Nuclear Energy (ORTN), National Research and Innovation Agency (BRIN), for the funding support that has been provided for the implementation of this research. This support is very valuable in enabling the implementation of research and development in the field of nuclear power.

AUTHOR CONTRIBUTION

N. Robifahmi contributed to methodology, laboratory analysis, data analysis, investigation, and writing the original draft. I. Sugoro contributed to conceptualization, methodology, and writing review and editing. R. I. Laksana, A. A. Pratama, A. T. Kusuma, V. A. Febrian, M. Yusup, W. Futy, and A. Mujiyanto contributed to laboratory analysis and gamma irradiation of samples. B. J. Tuasikal, T. Tjptosumirat, E. D. Nugraha, and M. S. Rijal contributed to writing review and editing. All authors read and approved the final version of the paper.

REFERENCES

1. M. Boezio, R. Munini, and P. Picozza, Prog. Part. Nucl. Phys. **112** (2020) 103765.
2. A. Mazzei-abba, C. L. Folly, C. Kreis *et al.*, J. Environ. Radioact. **239** (2021) 1.
3. N. Fathabadi, A. A. Salehi, K. Naddaf *et al.*, J. Environ. Radioact. **198** (2019) 11.
4. E. D. Nugraha, M. Hosoda, Y. Tamakuma *et al.*, J. Radioanal. Nucl. Chem. **330** (2021) 1437.
5. S. N. Shilfa, B. Y. E. B. Jumpeno, Nurokhim *et al.*, J. Phys. Conf. Ser. **1436** (2020) 012027.
6. I. Rosianna, E. D. Nugraha, H. Tazoe *et al.*, Geosci. **13** (2023) 388.

7. S. K. Shukla, A. Paraneeiswaran, and T. S. Rao, *J. Environ. Chem. Eng.* **8** (2020) 103549.
8. A. Wollenberg, J. Kretzschmar, B. Drobot *et al.*, *J. Hazard. Mater.* **411** (2021) 1.
9. A. D. Pratiwi, I. K. H. Basri, S. Purnami *et al.*, *Atom Indones.* **45** (2019) 103.
10. A. Abbasi and S. F. Mirekhtiary, *Eur. Phys. J. Plus* **135** (2020) 293.
11. E. D. Nugraha, J. Mellawati, Wahyudi *et al.*, *Toxics* **10** (1) (2022) 39.
12. Darlina, T. Rahardjo, H. N. E. Surniyantoro *et al.*, *Atom Indones.* **48** (2022) 21.
13. E. Soldi, C. Casey, B. R. Murphy *et al.*, *J. Fungi* **6** (2020) 1.
14. D. Ramadhani, S. Purnami, S. Nurhayati *et al.*, *Atom Indones.* **45** (2019) 27.
15. M. Cortesão, A. de Haas, R. Unterbusch *et al.*, *Front. Microbiol.* **11** (2020) 1.
16. M. C. Ogwu, S. Srinivasan, K. Dong *et al.*, *Environ. Microbiol.* **78** (2019) 855.
17. S. Freed, R. F. Ramaley, and J. A. Kyndt, *Microbiol. Resour. Announc.* **8** (2019) 1.
18. D. Neina, *Appl. Environ. Soil Sci.* **2019** (2019) 1.
19. Z. Liu, W. Zang, R. Ma *et al.*, *Commun Earth Environ.* **4** (2023) 1.
20. D. Billi, C. Staibano, C. Verseux *et al.*, *Astrobiol.* **19** (8) (2019) 1008.
21. I. Shuryak, *J. Environ. Radioact.* **196** (2019) 50.
22. J. C. Frisvad, V. Hubka, C. N. Ezekie *et al.*, *Stud. Mycol.* **93** (2019) 1.
23. I. Shuryak, R. Tkavc, V. Y. Matrosova *et al.*, *Sci. Rep.* **9** (2019) 1.
24. M. Kelley, M. J. Paulines, G. Yoshida *et al.*, *PLoS One* **17** (2022) 1.
25. Z. Schultzhaus, J. Romsdahl, A. Chen *et al.*, *Environ. Microbiol.* **22** (2020) 1310.
26. I. Jiménez-Gómez, G. Valdés-Muñoz, A. Moreno-Ulloa *et al.*, *Front. Microbiol.* **13** (2022) 1.
27. L. Liu, J. Chen, F. Liu *et al.*, *Environ. Res.* **194** (2021) 110691.
28. B.-B. Chi, Y.-N. Lu, P.-C. Yin *et al.*, *Front. Microbiol.* **12** (2021) 1.
29. N. Kolhe, S. Zinjarde, and C. Acharya, *J. Hazard. Mater.* **381** (2020) 121226.
30. E. Priyadarshini, S. S. Priyadarshini, B. G. Cousins *et al.*, *Chemosphere* **274** (2021) 129976.
31. E. Coelho, T. A. Reis, M. Cotrim *et al.*, *Chemosphere* **248** (2020) 126068.
32. C. Medina-Armijo, D. Isola, J. Illa *et al.*, *J. Fungi* **10** (2024) 1.
33. R. S. Ahmed, *Environ. Forensics* **22** (2021) 91.
34. P. P. Akhila, K. V. Sunooj, B. Aaliya *et al.*, *Trends Food Sci. Technol.* **114** (2021) 399.
35. P. C. Singh, S. Srivastava, D. Shukla *et al.*, *Mycoremediation Mechanisms for Heavy Metal Resistance/Tolerance in Plants*, in: *Mycoremediation and Environmental Sustainability Vol. II*, Springer, India (2018) 351.